Acta Oceanol. Sin., 2022, Vol. 41, No. 6, P. 88–98
https://doi.org/10.1007/s13131-021-1919-7
http://www.aosocean.com
E-mail: ocean2@hyxb.org.cn

Fluxes of riverine nutrient to the Zhujiang River Estuary and its potential eutrophication effect

Li Zhang[1, 3, 4], Yumin Yang[5], Weihong He[1, 3, 4], Jie Xu[2, 3, 4, 6], Ruihuan Li[2, 3, 4*]

[1] Marine Environmental Testing Center, South China Sea Institute of Oceanology, Chinese Academy of Sciences, Guangzhou 510301, China

[2] State Key Laboratory of Tropical Oceanography, South China Sea Institute of Oceanology, Chinese Academy of Sciences, Guangzhou 510301, China

[3] Southern Marine Science and Engineering Guangdong Laboratory (Guangzhou), Guangzhou 511458, China

[4] Innovation Academy of South China Sea Ecology and Environmental Engineering, Chinese Academy of Sciences, Guangzhou 510301, China

[5] Guangdong Environmental Monitoring Center, Guangzhou 510308, China

[6] College of Marine Science, University of Chinese Academy of Sciences, Qingdao 266404, China

Received 1 April 2021; accepted 15 June 2021

Abstract

The Zhujiang River Estuary is becoming eutrophic due to the impact of anthropogenic activities in the past decades. To understand nutrient dynamics and fluxes to the Lingdingyang water via four outlets (Humen, Jiaomen, Hongqimen and Hengmen), we investigated the spatial distribution and seasonal variation of dissolved nutrients in the Zhujiang River Estuary, based on fourteen cruises conducted from March 2015 to October 2017, covering both wet (April to September) and dry (October to March next year) seasons. Our results showed that riverine fluxes of dissolved inorganic nitrogen (DIN) and dissolved silicate (DSi) into the Lingdingyang water through four outlets varied seasonally due to the influence of river discharge, with the highest in spring and the lowest in winter. However, riverine flux of phosphate exhibited little significant seasonal variability. Riverine nutrients into the Lingdingyang water most resulted through Humen Outlet. The estuarine export fluxes of DIN out of the Zhujiang River Estuary derived from a box model were higher than fluxes of riverine nutrients in May, likely due to the influence of local sewage, while lower than riverine flux in August. The export fluxes of phosphate were higher than the fluxes of riverine phosphate in May and August. In contrast, large amounts of DSi were buried in the estuary in May and August. Although excess DIN was delivered into the Zhujiang River Estuary, eutrophication effect was not as severe as expected in the Zhujiang River Estuary, since the light limitation restricted the utilization of nutrients by phytoplankton.

Key words: riverine nutrient, flux, Lingdingyang, Zhujiang River Estuary, eutrophication

Citation: Zhang Li, Yang Yumin, He Weihong, Xu Jie, Li Ruihuan. 2022. Fluxes of riverine nutrient to the Zhujiang River Estuary and its potential eutrophication effect. Acta Oceanologica Sinica, 41(6): 88–98, doi: 10.1007/s13131-021-1919-7

1 Introduction

The massive anthropogenic activities have dramatically increased the loading of riverine nutrients on a global scale (Nixon, 1995). Increasing nutrient export from land to sea is considered as an important source of coastal pollution (Wang et al., 2006; http://www.nmdis.org.cn/hygb/zghyhjzlgb/). Riverine nutrient input leads to nutrient enrichment in estuarine and coastal waters, simulating primary production and causing hypoxic events (Turner and Rabalais, 1994; Cloern, 2001; Rabalais et al., 2007; Liang and Xian, 2018), which is recognized as a major threat to ecosystems (Billen and Garnier, 2007). For example, increasing nutrient export out of the Changjiang River Estuary has resulted in eutrophication in coastal waters of the East China Sea and increases the frequency of algal blooms (Qu and Kroeze, 2010). Hypoxia in the northern Gulf of Mexico is driven by the increased input of nutrients from Mississippi River (Malakoff, 1998).

The Zhujiang River (ZJR) is the third longest river (2 200 km) in China with a drainage area of 453 700 km^2. The ZJR Estuary (ZJRE) is located within the subtropical monsoonal climate zone with annual rainfall of 1 600–2 300 mm (Huang et al., 2003). The physical and biogeochemical processes in the ZJRE system vary seasonally due to the exchange between southwesterly and northeasterly monsoon wind and seasonal variations of river discharge (Huang et al., 2003). The annual river discharge from the ZJR is approximately 3.3×10^{11} m^3/a, 70%–80% of which occurs

Foundation item: The Special Project for Marine Economic Development (Six Major Marine Industries) of Guangdong Province under contract No. GDNRC[2020]064; the Key Special Project for Introduced Talents Team of Southern Marine Science and Engineering Guangdong Laboratory (Guangzhou) under contract Nos GML2019ZD0303, GML2019ZD0305 and GML2019ZD0402; the Innovation Academy of South China Sea Ecology and Environmental Engineering, Chinese Academy of Sciences under contract Nos ISEE2019ZR02 and ISEE2019ZR03; the National Natural Science Foundation of China under contract Nos 41676075 and 41706085; the Department of Science and Technology of Guangdong Province under contract No. 2018B030320005.
*Corresponding author, E-mail: lirh@ysfri.ac.cn

from April to September (wet season) and 20%–30% from October to March (dry season) (Wei and Wu, 2014). The ZJR discharges to the South China Sea (SCS) through three waters, Lindingyang (LDY), Modaomen and Huangmaohai (Fig. 1). This study will focus on LDY, the principal estuary of the ZJR, which is traditionally known as the ZJRE (Cai et al., 2004). It is estimated that the ZJRE receives 50%–55% of the ZJR freshwater discharge through four outlets (Humen (HM), Jiaomen (JM), Hongqimen (HQM) and Hengmen (HeM)) (Cai et al., 2004).

The ZJR delta region is located in a highly populated and economically developed region. The discharge of industrial and domestic wastewater in Guangdong Province increased from 4.48×10^{10} t/a in 2 000 to 9.04×10^{10} t/a in 2018 due to economic development (http://stats.gd.gov.cn/). Large amounts of nutrients are delivered to the LDY through four outlets (Harrison et al., 2008; Dai et al., 2014). The concentrations of dissolved inorganic nitrogen (DIN) in the ZJR delta have increased from 110 μmol/L in 1984 to 149 μmol/L (Lu et al., 2009). Nitrate (NO_3^-) concentrations in the ZJR are extremely high (up to 100 μmol/L) (Xu et al., 2008b), while phosphate concentrations are relatively low (~1 μmol/L), resulting in high N:P concentration ratio in the ZJRE, ranging from ~30 in the lower estuary to over 100 in the upper estuary (Huang et al., 2003; Harrison et al., 2008). P limitation might restrict N utilization by phytoplankton. Meanwhile, eutrophication and hypoxia have emerged in the estuarine and coastal waters and become an issue of concern (Dai et al., 2014; Qian et al., 2018; Li et al., 2020). Much attention has been paid to tempo-spatial in the nutrient levels (Cai et al., 2004; He et al., 2014; Li et al., 2017), nutrient fluxes at the sediment-water interface (Zhang et al., 2014), export fluxes of nutrients from the ZJRE to coastal water (Liu, 2006; Liu et al., 2009), fluxes of riverine nutrients from the river network based on physical-biological model (Hu and Li, 2009; Hu et al., 2012; Gan et al., 2014), physical processes (Cai et al., 2018; Gong et al., 2018) and harmful algal blooms (Tang et al., 2003; Lu and Gan, 2015) in the ZJRE. However, little was known the fluxes of riverine nutrients via various outlets to the ZJRE, which was important to quantify the contribution of riverine nutrients to the nutrient inventory in the estuary.

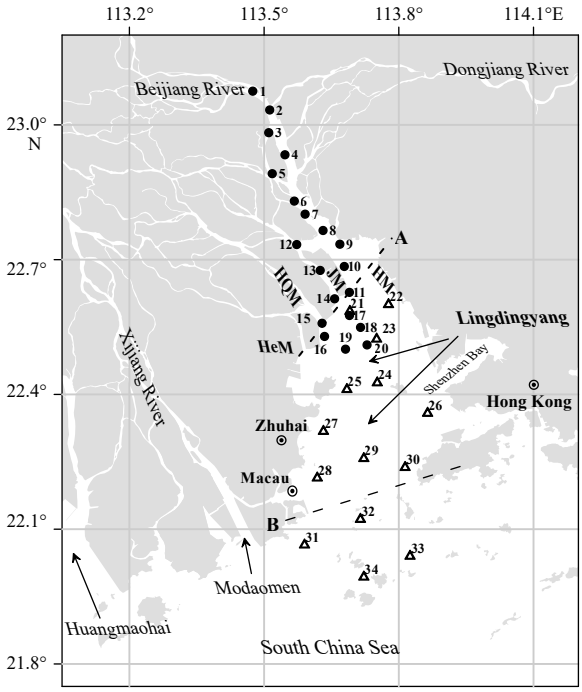

Fig. 1. Location of sampling stations in the Zhujiang River Estuary during March 2015–October 2017. The solid circles denoted the sampling stations 1–20 during March 2015–October 2017; triangles, sampling stations 21–34 in May and August 2015. HM, JM, HQM and HeM represented the Humen, Jiaomen, Hongqimen and Hengmen, respectively. Dashed Line A was the boundary of riverine flux to the Lingdingyang water via four outlets; Line B showed the boundary of the budget systems as previous study (Liu et al., 2009).

The objectives of the present study were to quantify riverine nutrient fluxes to the LDY through four outlets on the seasonal basis, and to assess potential eutrophication effects induced by riverine nutrients in the ZJRE.

2 Materials and methods

2.1 *Study area*

The ZJRE was divided into three zones following previous studies (Dai et al., 2014; Guo et al., 2009). The upstream of HM Outlet was defined as the upper estuary, the inner LDY as the middle estuary and the region in the outer LDY as the lower estuary (Fig. 1). Cruises were carried out in the upper reach of the ZJRE and the top of the LDY (Stations 1 to 20 for each cruise) which stretched from the HM Outlet upward to the suburbs of Guangzhou on the seasonal basis (March, May, August and October) during 2015–2017 and in the middle and lower parts of the ZJRE (Stations 21–34) in May and August 2015 (Fig. 1). Salinity and temperature were determined by a Seabird 911 plus conductivity-temperature-depth (CTD). Samples for nutrients, chlorophyll *a* (Chl *a*) and dissolved oxygen (DO) concentrations were taken at the surface.

The determination of nitrite (NO_2^-) is based on the reaction of NO_2^- with an aromatic amine, and the product is quantified by spectrophotometry (Hansen and Koroleff, 1999). NO_3^- and ammonium (NH_4^+) were determined using the Cu-Cd column reduction method and the indophenol blue color formation, respectively (Hansen and Koroleff, 1999). The concentration of DIN was the sum of NO_3^-, NO_2^- and NH_4^+. Dissolved inorganic phosphate (DIP) was measured by the ascorbic acid method (Hansen and Koroleff, 1999). Dissolved silicate (DSi) was analyzed using molybdate, oxalic acid and a reducing reagent (Hansen and Koroleff, 1999). The analytical precision for NO_3^-, NO_2^-, NH_4^+, DIP and DSi was <5%.

Chl *a* was extracted in 10 mL of 90% (*v*/*v*) acetone at 4°C in the dark for 14–24 h and then determined before and after the acidification with 1 μmol/L HCl using a Turner designs Trilogy fluorometer (Parsons et al., 1984). DO concentration was determined using the Winkler method (Oudot et al., 1988).

2.2 *Estimation of riverine nutrient fluxes into the estuary*

2.2.1 *Riverine nutrient fluxes into the estuary*

Based on nutrient concentrations of the freshwater end-members and on the assumption that the nutrients remained in a steady state during the investigation, we used Eq. (1) to calculate the riverine fluxes through the outlet into the estuary:

$$F = CQ, \tag{1}$$

where F is the flux of each nutrient species during investigation;

C is nutrients concentration in the freshwater end-member; Q is the freshwater discharge during the study periods (March 2015–October 2017) which was obtained from http://www.pearl-water.gov.cn/. HM, JM, HQM and HeM provide 35%, 33%, 20% and 12% of the bulk freshwater discharge of the ZJR, respectively (Kot and Hu, 1995).

2.2.2 *Export fluxes of nutrients from the estuary into the sea*

Dissolved nutrient budgets for the study system were constructed based on the Land-Ocean Interactions in the Coastal Zone box model (Gordon et al., 1996). This model has been widely used to construct nutrient budgets defining the internal biogeochemical processes (e.g., denitrification) and external nutrient inputs of estuarine and coastal ecosystems (Savchuk, 2005; Liu et al., 2009). In this model, the study system is assumed to be single box, which is well-mixed and assumed to be at a steady state. Taking salinity as 0 for fresh water (water from the river discharge, rainfall and evaporation), therefore, the water mass balance and salinity balance based on water budgets were estimated according to Eqs (2) and (3), respectively:

$$V_{\mathrm{R}} = V_{\mathrm{in}} - V_{\mathrm{out}} = -V_{\mathrm{Q}} - V_{\mathrm{P}} - V_{\mathrm{G}} - V_{\mathrm{W}} + V_{\mathrm{E}}, \quad (2)$$

$$V_{\mathrm{X}}(S_1 - S_2) = S_{\mathrm{R}} V_{\mathrm{R}}, \quad (3)$$

where V_{R} is the residual water flow exported from the estuary into the adjacent coastal zone, and V_{Q}, V_{P}, V_{G}, V_{W}, V_{E}, V_{in}, V_{out} and V_{X} are the river discharge, precipitation, groundwater, wastewater, evaporation, inflow of water to the system of interest, outflow of water from the system of interest and the mixing flow between the system of interest and adjacent system, respectively. In Eq. (3), $S_{\mathrm{R}} = (S_1 + S_2)/2$, where S_1 and S_2 are the average salinity of the system of interest and the adjacent system, respectively.

For the water budget, the daily precipitation and evaporation in the wet season were estimated using the following equations:

$$V_{\mathrm{P}} = 80\% \times a \times H/t, \quad (4)$$

$$V_{\mathrm{E}} = 63\% \times a \times H/t, \quad (5)$$

where a denoted the area of the ZJRE, which is reported to be 1 180 km^2 (Liu et al., 2009). H denoted rainfall or evaporation, t denoted the days of the wet season. Precipitation is significantly correlated with the water discharge (Dai et al., 2014). The 80% of the ZJR discharge occurs in the wet season (Huang et al., 2003). Hence, it was assumed that 80% of the annual rainfall took place in the wet season (April to September). The evaporation in winter was approximately accounted for 60% of the evaporation in summer (Liu et al., 2009). Thus, it was assumed that the evaporation in the dry season was accounted for 60% of the evaporation in the wet season. Hence, it was estimated that 63% of the annual evaporation took place in the wet season. Previous study pointed out that the section from the HM Outlet upward to Guangzhou received most of the waste water and sewage discharged from Guangzhou (Dai et al., 2006). Hence, sewage discharge (V_{W}) was included in river discharge to compute the water budget of the estuary. Groundwater (V_{G}) in Chinese rivers and coastal areas contributed to a small fraction of nutrient fluxes (Liu et al., 2009). In addition, recirculated seawater could account for 75% to 90% of the bulk submarine groundwater discharge (Moore, 1996; Beck et al., 2008), which increases with precipitation (Guo et al., 2008). Hence, V_{G} is negligible in the calculation of the water budget. The residual flow (V_{R}) was calculated from the sum of ($-V_{\mathrm{Q}} - V_{\mathrm{P}} + V_{\mathrm{E}}$) as a result.

Non-conservative fluxes of nutrient can be derived based on water budgets and nutrient concentrations (Fig. 2). Nutrient fluxes from the estuary to the adjacent system were estimated as the sum of the net residual flux ($V_{\mathrm{R}}C_{\mathrm{R}}$) and the mixing flux ($V_{\mathrm{X}}C_{\mathrm{X}}$) (Fig. 2), where C_{R} is the average element concentration in the residual flow boundary, $C_{\mathrm{R}} = (C_1 + C_2)/2$; C_{X} is the mixing flow, $C_{\mathrm{X}} = (C_1 - C_2)/2$. C_1 and C_2 are the average nutrient concentrations of the estuary and the adjacent system, respectively. The difference (Δ) between the sum of ($V_{\mathrm{R}}C_{\mathrm{R}} + V_{\mathrm{X}}C_{\mathrm{X}}$) and the riverine input ($F = CQ$) was used to estimate the estuarine processes that may magnify the riverine flux (Fig. 2).

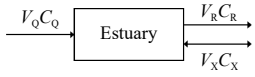

Fig. 2. Total Nutrient flux (residual flux ($V_{\mathrm{R}}C_{\mathrm{R}}$) and mixing exchange flux ($V_{\mathrm{X}}C_{\mathrm{X}}$)) from the Zhujiang River Estuary to the South China Sea derived from box model and riverine input ($V_{\mathrm{Q}}C_{\mathrm{Q}}$) to the estuary.

2.3 *Statistical analysis*

Statistical analyses were performed using the software SPSS 20.0 by IBM. The Pearson's correlation efficient was performed to determine the correlation between two variables at the level of p<0.05. The independent t-test was employed to compare in difference between two variables at the level of p<0.05. ANOVA was used to analyze the individual effects of seasons on variations in nutrient concentrations at the level of p<0.05.

3 Results and discussion

3.1 *Spatial and temporal variations in nutrient concentrations*

Temperature and salinity exhibited clear seasonal variability (Fig. 3, Table 1) (p<0.05). In the wet season (May and August), salinity at Station 1 to Station 20 was low (0.08–7.41, the average of 0.54). In the dry season (March and October), salinity increased from Station 1 to Station 11 (Fig. 3). Salinity in the wet season was significantly (p<0.05) lower than in the dry season. Similarly, discharge was higher in the wet season than the dry season (p<0.05) (Table 1). Temperature was the highest (23.9–28.6°C) in summer (August), followed by spring (13.6–27.9°C) and fall (25.8–28.6°C), the lowest (18.7–21.6°C) in winter (March) (Table 1) (p<0.05).

The highest NO_3^- and NH_4^+ concentrations (up to 270 μmol/L for NO_3^- and 180 μmol/L for NH_4^+) occurred in waters (Station 1 and Station 2) near the HM Outlet. In general, NO_3^- concentrations were significantly higher ((141.0±44.3) μmol/L) in the dry season (March and October) than those ((117.0±33.1) μmol/L) in the wet season (May and August) (p<0.05) (Fig. 4). NH_4^+ concentrations reached the highest ((147.0±35.7) μmol/L) in March. In contrast, DSi concentrations were generally higher ((278.0±85.2) μmol/L) in the wet season (May and August) than the dry season ((228.0±89.1) μmol/L) (Fig. 4). The highest DSi concentration ((313.0±65.8) μmol/L) occurred in spring (May) among four seasons, when the river discharge reached a peak (Fig. 4 and Table 1). DIP concentrations were higher ((2.20±1.91) μmol/L) in the dry season (March and October) than those ((1.44±0.85) μmol/L) in the wet season (May and August) (p<0.05) (Fig. 4). However, DIP showed the different pattern from DIN. The DIP concentrations were the highest ((2.65±2.26) μmol/L) in October and the lowest ((1.16±0.55) μmol/L) in May (p<0.05) (Fig. 4). DIN:DIP concentration ratios were generally more than 100:1 (Fig. 5), suggesting

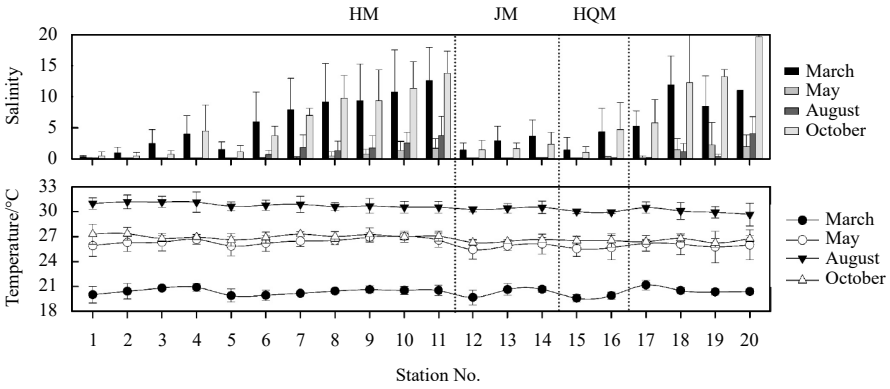

Fig. 3. Spatial and temporal variations in the surface salinity and temperature in the Zhujiang River Estuary during March 2015–October 2017. Vertical bars denoted standard deviation errors. HM, JM and HQM represented the Humen, Jiaomen and Hongqimen, respectively.

Table 1. Discharge, temperature and salinity at Stations 1–20 during March 2015–October 2017. The average values were shown in parentheses

Month	Discharge/($m^3 \cdot s^{-1}$)	Temperature/°C	Salinity
March	3 669–9 904 (7 296)	18.7–21.6 (20.4)	0.13–16.7 (5.66)
May	10 383–19 700 (15 480)	23.6–27.9 (26.2)	0.08–1.99 (0.30)
August	12 866–16 938 (14 968)	28.6–32.1 (30.6)	0.08–7.41 (0.79)
October	11 855–15 034 (13 367)	25.8–28.6 (26.8)	0.11–21.4 (5.90)

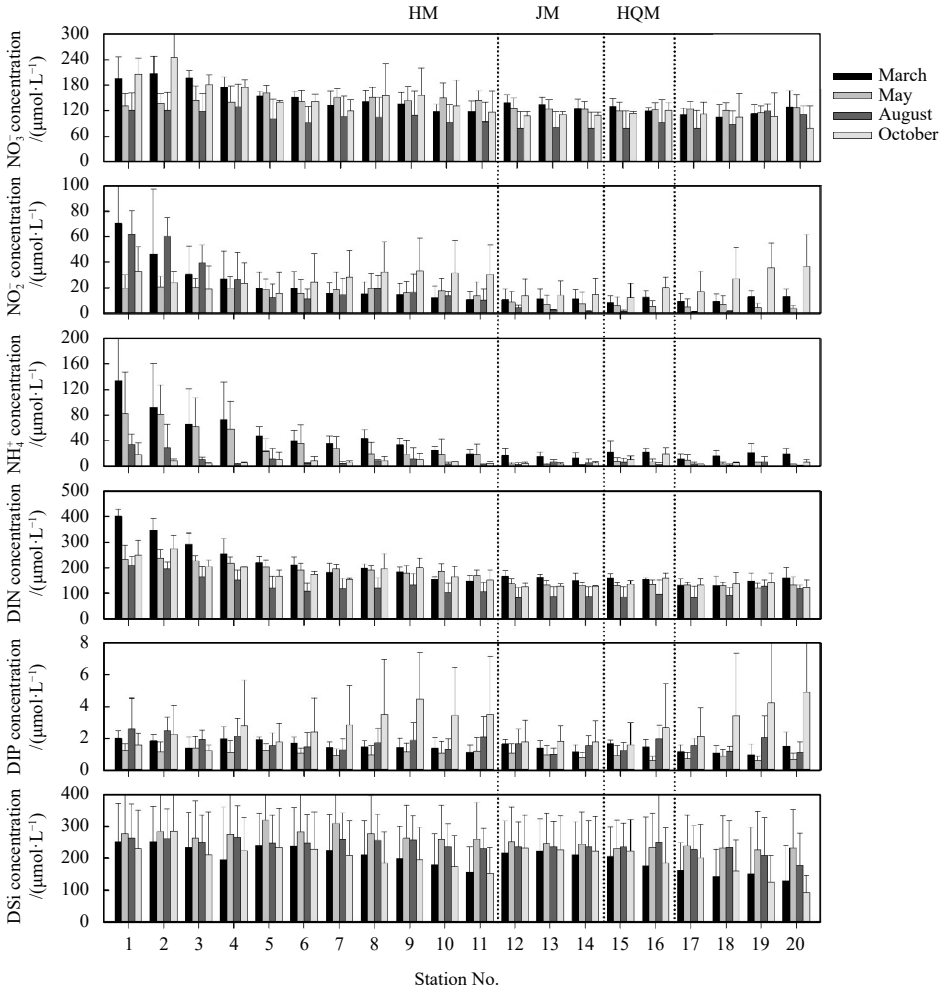

Fig. 4. Spatial and temporal variations in the surface NO_3^-, NO_2^-, NH_4^+, DIN, DIP and DSi concentrations in the Zhujiang River Estuary during March 2015–October 2017. Vertical bars denoted standard deviation errors. HM, JM and HQM represented the Humen, Jiaomen and Hongqimen, respectively.

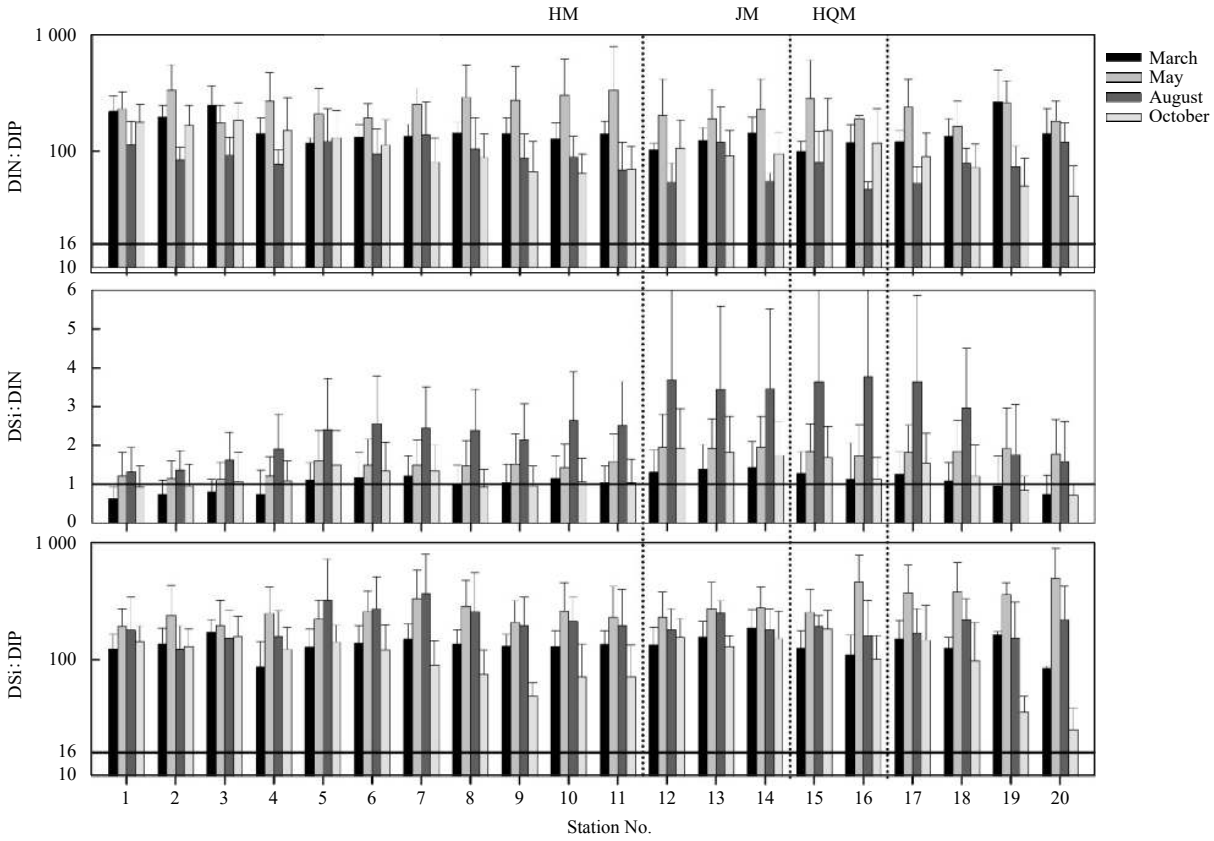

Fig. 5. Monthly average concentration ratios of DIN:DIP, DSi:DIN and DSi:DIP at the sea surface at Stations 1–20 during March 2015–October 2017. Vertical bars denoted standard deviation errors. HM, JM and HQM represented the Humen, Jiaomen and Hongqimen, respectively.

that P was potentially limiting phytoplankton growth in the study area, in agreement with the early reports (Xu et al., 2008b). Similarly, high N:P concentration ratio is also reported in the Changjiang River Estuary (Liang and Xian, 2018). DSi:DIN concentration ratios were higher in the wet season than the dry season due to relatively high concentration of DSi (Fig. 5).

Temporal variability in NO_3^-, DIN and DSi concentrations was obvious in the ZJR (Fig. 6). The concentrations of NO_3^-, DIP and DSi declined from the middle to lower estuary (Fig. 6). Both DIN and DSi had a significant (p<0.05) relationship with salinity (Fig. 6). Chl *a* concentration was the highest in August ((17.2±12.3) μg/L) and the lowest in May ((11.4±9.34) μg/L) (Fig. 7a). The concentration of Chl *a* could reached a peak ((50.4±15.1) μg/L) at Station 2 in October.

In general, surface DO concentration was higher ((5.77±1.96) mg/L) in the dry season than that ((4.91±1.86) mg/L) in the wet season, especially in HM channel (Fig. 7b). The lowest surface DO was 0.77 mg/L in March at Stations 1 and 2 (Fig. 7b). Surface DO concentration increased gradually from suburbs of Guangzhou to HM Outlet and upper reach of the LDY, in agreement with previous reports (Dai et al., 2006; He et al., 2014). In the dry season, seawater could intrude up to 50 km of the upstream of HM Outlet (Harrison et al., 2008). The seawater-freshwater mixing resulted in a seaward increase in DO in the dry season when DO rich seawater intruded the upper reach of the LDY (Figs 3 and 7b). In addition, the highest rate of the total oxygen consumption normalized to the substrate was observed in summer (He et al., 2014), which might also lead to the lower level of DO in the wet season.

3.2 *Riverine nutrient fluxes to the Lingdingyang water via four outlets*

The fluxes of DIN and DSi to LDY via four outlets varied seasonally (Table 2). The fluxes of DIN and DSi reached a peak ((6.37±1.67)×10^7 mol/d for DIN and (9.68±3.73)×10^7 mol/d for DSi via the HM Outlet, (3.30±0.76)×10^7 mol/d for DIN and (7.65±2.58)×10^7 mol/d for DSi via the JM Outlet, (1.10±0.38)×10^7 mol/d for DIN and (2.60±0.95)×10^7 mol/d for DSi via the HQM Outlet, 1.98×10^7 mol/d for DIN via the HeM Outlet) in spring. In contrast, the lowest fluxes of DIN and DSi ((2.50±0.99)×10^7 mol/d for DIN and (2.47±1.21)×10^7 mol/d for DSi via the HM Outlet, (1.23±0.45)×10^7 mol/d for DIN and (2.05±0.84)×10^7 mol/d for DSi via the JM Outlet, (0.45±0.16)×10^7 mol/d for DIN and (0.71±0.28)×10^7 mol/d for DSi via the HQM Outlet, 0.55×10^7 mol/d for DIN via the HeM Outlet) occurred in winter (Table 2) (p<0.05).

Riverine nutrient fluxes via four outlets differed. Nutrient fluxes via the HM Outlet were the highest (1.57×10^5 t/a for NO_3^-, 2.30×10^5 t/a for DIN, 1.11×10^3 t/a for DIP, 3.03×10^5 t/a for DSi) among four outlets, followed by the JM and HeM outlets, the lowest (3.84×10^4 t/a for NO_3^-, 4.36×10^4 t/a for DIN, 4.80×10^2 t/a for DIP, 8.82×10^4 t/a for DSi) for the HQM Outlet (Table 3) (p<0.05).

The difference in nutrient fluxes was primarily attributed to different river discharge. The fluxes of NO_3^-, DIN and DSi were significantly (p<0.05) correlated with river discharge, rather than DIP (Fig. 8). Seasonality in the river discharge was responsible for seasonal variability in nutrient fluxes to the LDY (Table 2). The maximum nutrient fluxes of DIN and DSi in spring were related to the highest river discharge. However, fluxes of DIP lacked seasonality (Table 2). Furthermore, NO_3^- was significantly (p<0.05)

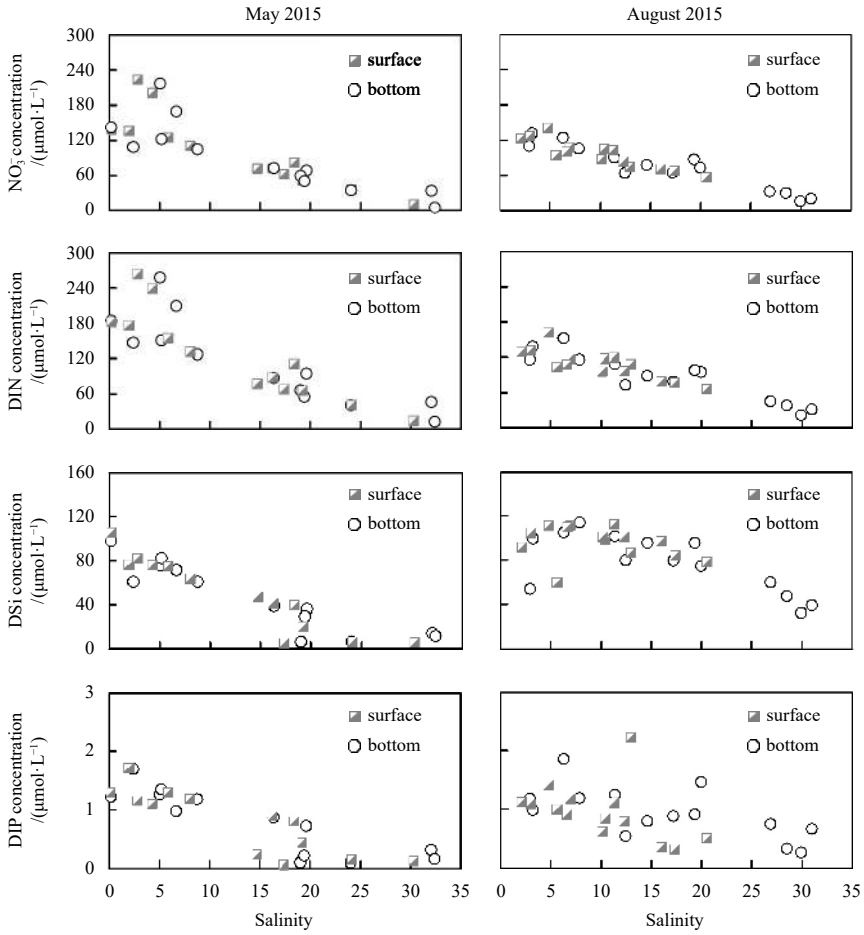

Fig. 6. Variations in the concentrations of NO_3^-, DIN, DSi and DIP along a salinity gradient in the Zhujiang River Estuary at the sea surface and the sea bottom at Stations 21–34 in May and August 2015.

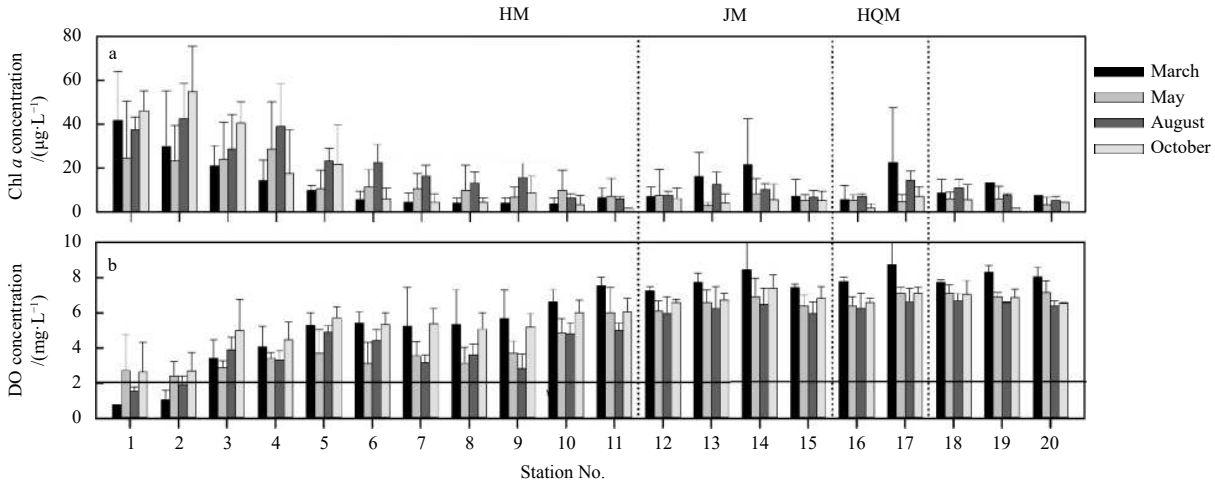

Fig. 7. Spatial and temporal variations in chlorophyll *a* (Chl *a*) (a) and dissolved oxygen (DO) (b) concentrations at the sea surface during March 2015–October 2017. The solid line in b represented the value of DO equalled to 2 mg/L. Vertical bars denoted standard errors. HM, JM and HQM represented the Humen, Jiaomen and Hongqimen, respectively.

correlated with DSi, while DIP was not significantly correlated with NO_3^- and DSi, respectively (Fig. 9). These results suggested that NO_3^- and DSi primarily resulted from the watershed while DIP most likely originated from the local sewage. Our results agreed with previous reports that the river discharge delivered NO_3^- and DSi (Yin et al., 2000; Xu et al., 2008b) and P results from the point sources of industrial and domestic waste (Zhang et al., 1995; Strokal et al., 2015).

There was a significant (p<0.05) correlation between NO_3^- and DIN in three seasons (March, August and October) (Fig. 10). In

Table 2. Estimation of nutrient fluxes (Mean±SD) via four outlets in four seasons

	Discharge/($m^3 \cdot s^{-1}$)	$F_{NO_3^-}$/(10^6 mol·d^{-1})	F_{DIN}/(10^6 mol·d^{-1})	F_{DIP}/(10^6 mol·d^{-1})	F_{DSi}/(10^6 mol·d^{-1})	F_{DIN}:F_{DIP}	F_{DSi}:F_{DIN}	F_{DSi}:F_{DIP}
Humen								
March	947	15.0 ± 3.01	25.0 ± 9.90	0.17 ± 0.05	24.7 ± 12.1	148	1.00	150
May	3 302	36.2 ± 15.8	63.7 ± 16.7	0.13 ± 0.03	96.8 ± 37.3	490	1.52	744
August	3 146	35.6 ± 12.5	49.6 ± 11.9	0.19 ± 0.10	69.7 ± 30.0	255	1.41	359
October	2 229	36.7 ± 5.72	42.4 ± 4.37	0.38 ± 0.24	46.3 ± 27.1	113	1.09	124
Jiaomen								
March	893	10.7 ± 4.54	12.3 ± 4.54	0.11 ± 0.05	20.5 ± 8.41	109	1.67	183
May	3 114	30.0 ± 8.47	33.0 ± 7.60	0.26 ± 0.04	76.5 ± 25.8	124	2.32	289
August	2 966	23.0 ± 12.4	24.2 ± 12.7	0.38 ± 0.16	58.5 ± 23.3	63.0	2.42	152
October	2 101	19.8 ± 2.10	22.9 ± 1.29	0.33 ± 0.22	41.8 ± 21.0	69.7	1.82	127
Hongqimen								
March	325	3.75 ± 1.65	4.51 ± 1.62	0.05 ± 0.03	7.05 ± 2.84	90.3	1.56	141
May	1 132	10.5 ± 4.02	11.0 ± 3.81	0.11 ± 0.04	26.0 ± 9.51	114	2.17	248
August	1 078	8.40 ± 4.80	8.80 ± 4.87	0.12 ± 0.04	21.2 ± 7.96	75.8	2.41	183
October	764	7.49 ± 0.70	8.93 ± 0.44	0.11 ± 0.09	14.9 ± 7.06	83.6	1.67	140
Hengmen[a]								
March	541	3.80	5.48	0.04	N/A	138	N/A	N/A
May	1 887	16.3	19.8	0.13	N/A	150	N/A	N/A
August	1 797	16.6	20.5	0.16	N/A	130	N/A	N/A
October	1 274	10.9	12.7	0.11	N/A	111	N/A	N/A

Note: N/A means no data; a, data from Liu (2006).

Table 3. Summary of the yearly average nutrient flux (10^3 t/a)

	$F_{NO_3^-}$	F_{DIN}	F_{DIP}	F_{DSi}
Humen	157	230	1.11	303
Jiaomen	106	118	1.39	251
Hongqimen	38.4	43.6	0.48	88.2
Hengmen	60.7	74.6	0.57	N/A
Riverine flux	362	466	3.55	N/A
Export flux	491	585	10.8	609

Note: N/A means no data.

contrast, NH_4^+ was significantly (p<0.05) correlated with DIN in March and May. Furthermore, the peak of NH_4^+ occurred in March (Fig. 10). NH_4^+ primarily originates from the local sewage, especially in the upstream in the surface waters (Dai et al., 2006), while NO_3^- comes from the agriculture (Turner and Rabalais, 1991; Strokal et al., 2015). These results indicated that N source of DIN changed seasonally, which was possibly linked to seasonal changes in anthropogenic activities (e.g., fertilization in agriculture and sewage discharge). It is also reported that nitrate concentrations in the Changjiang River likely are associated with the intensive agricultural activities over the drainage region (Zhang et al., 1995; Liang and Xian, 2018).

The flux ratio of DIN:DIP varies seasonally and with the outlets (Table 2). In the HM Outlet, the flux ratio of DIN:DIP was the highest among four outlets, likely owing to higher NO_3^- loading from the watershed, since N:P flux ratio of nutrients from agricultures is high while N:P flux ratio of nutrients in the sewage is less than Redfield ratio (Xu et al., 2008a). The discrepancy in N:P flux ratio corroborated the statement that nutrient sources were different through various outlets.

3.3 *The export fluxes of nutrients out of the Zhujiang River Estuary during the wet season*

The water budget was calculated according to Eq. (4), where the annual rainfall (1 845 mm/a) and evaporation (2 160 mm/a) data of Guangdong in 2015 (Statistical Bureau of Guangdong Province, 2015) were used. Thus, the daily water budgets derived from precipitation and evaporation both in May and August were estimated to 9.68×10^6 m^3/d and 9.33×10^6 m^3/d, respectively (Fig. 11). The bulk freshwater discharge (V_Q) into the ZJRE through four outlets during our observation period was 9 141 m^3/s in May and 6 572 m^3/s in August 2015, respectively (the water discharge data were collected from http://www.pearlwater.gov.cn/). Based on the water mass balance, the residual flow (V_R) from the estuary to the SCS was estimated to be 7.91×10^8 m^3/d in May and 5.69×10^8 m^3/d in August, respectively. The water exchange flow (V_X) between the SCS and the estuary was 6.64×10^8 m^3/d in May and 5.88×10^8 m^3/d in August, respectively (Fig. 11).

Nutrient fluxes from the estuary to the SCS were the sum of the net residual flux (V_RC_R) and the mixing flux (V_XC_X) based on the water budget (Fig. 2 and Table 4). The export fluxes of NO_3^-, DIN, DIP and DSi to the ZJRE were 1.21×10^8 mol/d, 1.49×10^8 mol/d, 1.05×10^6 mol/d and 5.97×10^7 mol/d in May, respectively (Table 4). The net fluxes of NO_3^-, DIN, DIP and DSi in May were -4.93×10^7 mol/d, -4.67×10^7 mol/d, -3.00×10^5 mol/d and 8.53×10^7 mol/d, respectively. These results suggested that the export fluxes of NO_3^-, DIN and DIP to the ZJRE exceeded the fluxes of nutrients to ZJR via four outlets except for DSi. Hence, extra nutrients (NO_3^-, DIN and DIP) most likely originated from the local sewage. Interestingly, the net flux of NO_3^- was more than DIN in May, implying that the quantity of riverine NH_4^+ loss induced by biological utilization or nitrification. Riverine NH_4^+ was transformed to NO_3^- in the ZJRE, leading to an increase in the net flux of NO_3^-, rather than the input of NO_3^-. In addition, NH_4^+ was preferentially taken up by phytoplankton over NO_3^- (McCarthy, 1981; Xu et al., 2012; Glibert et al., 2016). Riverine NH_4^+ loss induced by biological utilization resulted in a decline in the export flux of DIN out of the ZJRE, rather than NO_3^-, which might partly interpret higher net flux of NO_3^- than DIN.

In comparison, the export fluxes of NO_3^-, DIN, DIP and DSi out of the ZJRE were 7.18×10^7 mol/d, 8.04×10^7 mol/d, 8.60×10^5 mol/d and 6.00×10^7 mol/d in August, respectively. Furthermore, the export fluxes of NO_3^-, DIN, DIP and DSi were lower than the fluxes of nutrients to the ZJRE via four outlets. As a result, the net

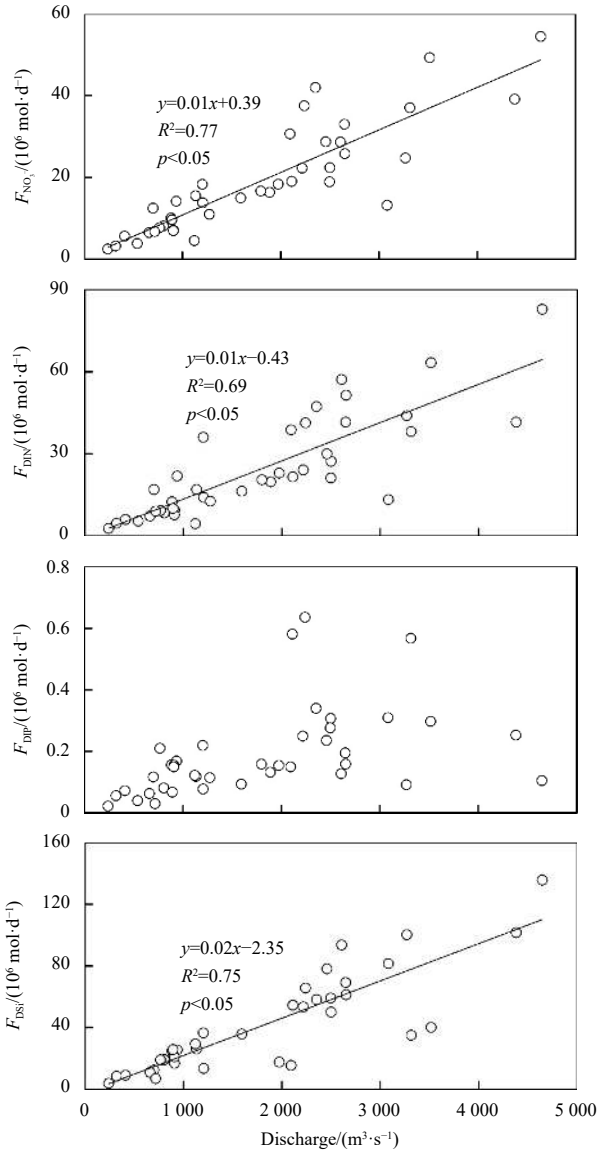

Fig. 8. Relationship between riverine nutrients fluxes to the Lingdingyang water via four outlets and the river discharge at the sea surface.

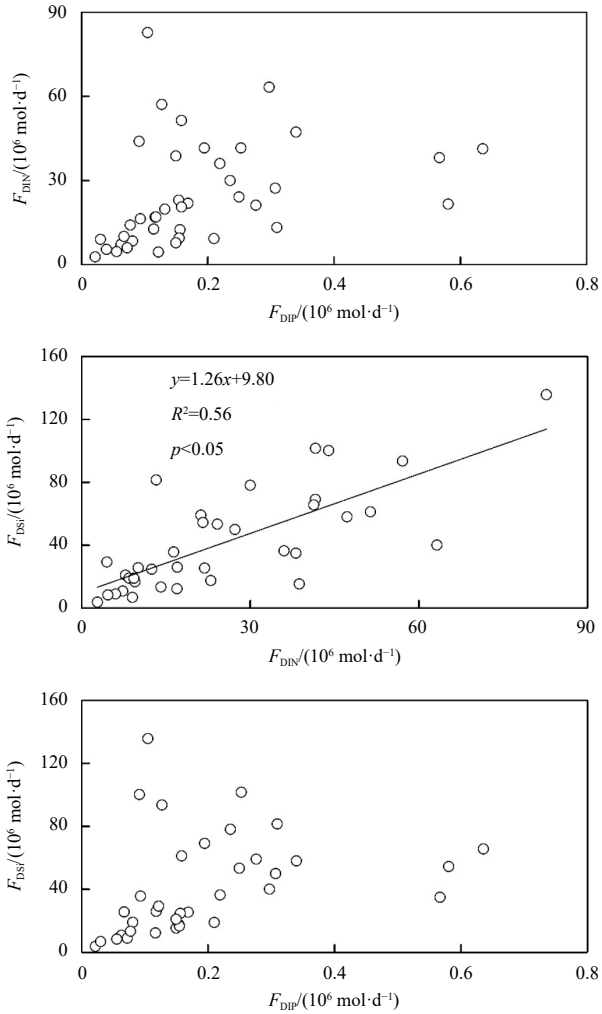

Fig. 9. The relationship of riverine nutrient fluxes at the sea surface at Stations 1–20 during March 2015–October 2017.

fluxes of NO_3^-, DIN, DIP and DSi in August were 3.60×10^6 mol/d, 1.07×10^7 mol/d, -8.00×10^4 mol/d and 1.10×10^8 mol/d, respectively (Table 4). This indicated that large amounts of NO_3^-, DIN and DSi were buried in the sediment or biologically utilized. The net fluxes of DSi did not follow the pattern of DIN and DIP, which were 8.53×10^7 mol/d and 1.10×10^8 mol/d in May and August, respectively.

In addition, the export fluxes of DIP out of the ZJRE were higher than the fluxes of DIP to the ZJRE via four outlets in May and August, indicating that DIP derived from local sewage which was possibly an important source of DIP in the ZJRE. N:P concentration ratio in the sewage is 8:1–10:1 (Xu et al., 2008a), less than the Redfield ratio (16:1). Hence, nutrient from the local sewage played an important role in regulating nutrient dynamics in the ZJRE (Xu et al., 2008a). Riverine DIN:DIP concentration ratios (Table 2) differed from the concentration ratio of N:P in the local sewage (8:1–10:1), which was responsible for the fact that the net export of DIP out of the ZJRE was distinct from DIN in August.

3.4 *Eutrophication effects in the ZJRE*

High loading of riverine nutrients has caused severe eutrophication in estuaries and coasts (Jickells, 1998). The river source was one of the most important sources through four outlets to LDY (Table 3). Large amounts of anthropogenic nutrients input led to nitrogen over-enrichment in the estuary and coastal region (Tables 3 and 4). Severe eutrophication effects, such as algal blooms and hypoxic events, occur in the ZJRE and adjacent coastal waters (Lu and Gan, 2015; Qian et al., 2018). Nutrient concentrations in the upper reach of the ZJRE (Fig. 4) were always greater than the half saturation constants (DIP: 0.1–0.5 μmol/L; DIN: 1–2 μmol/L; DSi: 1–5 μmol/L; Fisher et al., 1988) for nutrient uptake of phytoplankton. However, phytoplankton biomass was not as high as expected (Fig. 4). The maximum phytoplankton biomass was regulated by DIP availability in the ZJRE where P was the potential limiting nutrient. At Stations 1–20, the DIP and Chl *a* were on average 1.80 μmol/L and 14.7 μg/L during our study period, respectively. Assuming the ratio of Chl *a* : DIN concentration ratio (0.9 μg/μmol) (Yin et al., 1996) and Redfield ratio (16DIN:1DIP), Chl *a* concentrations reached 40.6 μg/L when DIP were converted to phytoplankton biomass. Therefore, nutrients were underutilized in the upper ZJRE. Our results were similar to previous observations (Yin and Harrison, 2008). Previous studies point out that suspended particulate matter (SPM) control primary productivity by reducing the light level

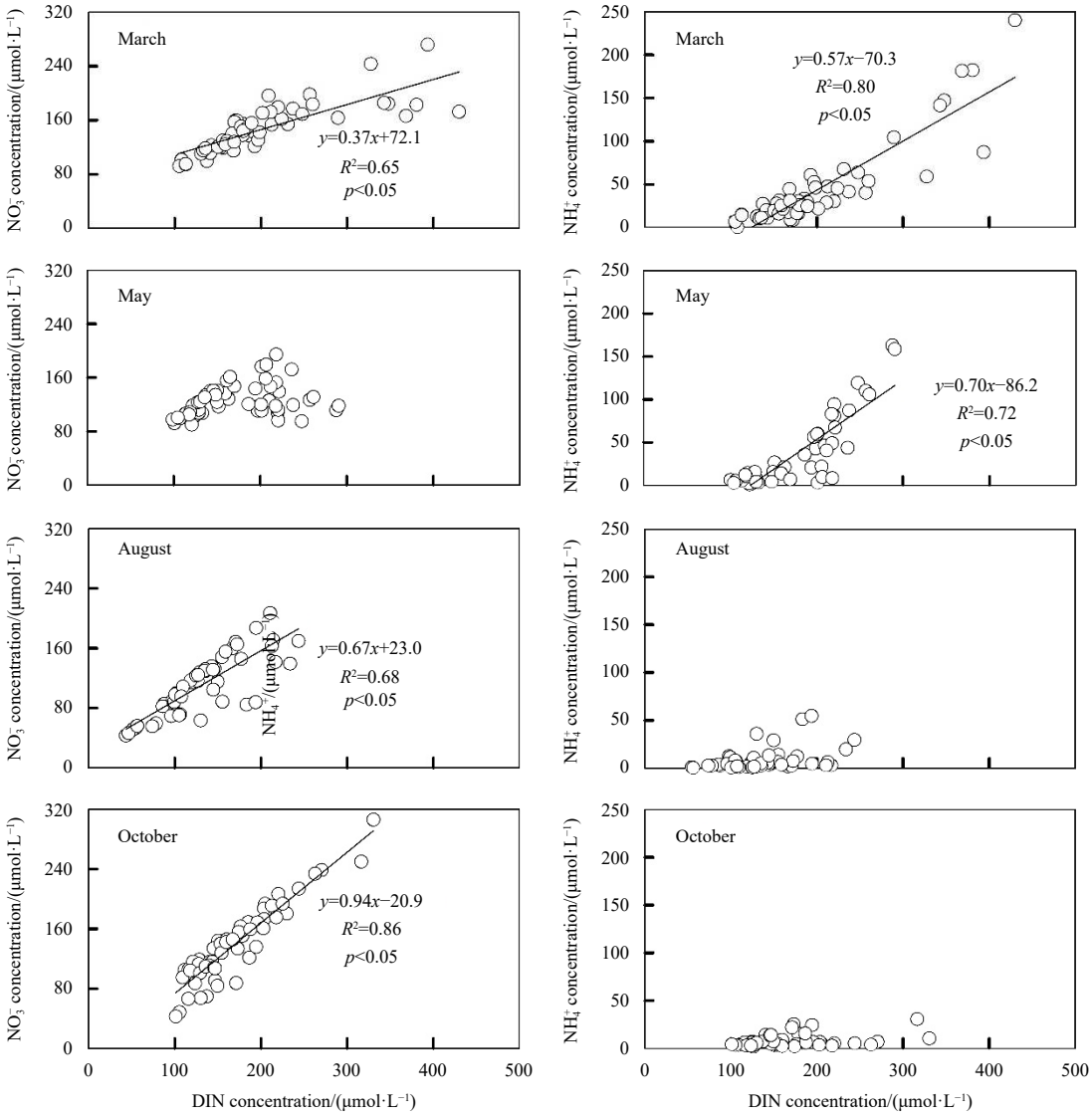

Fig. 10. Relationship between NO_3^- and DIN and relationship between NH_4^+ and DIN at the sea surface at Stations 1–20 from March 2015 to October 2017. The graphs with lines indicated significant correlation between the two variables, and the correlation coefficients were given in the graphs.

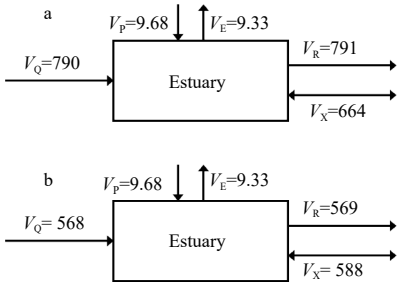

Fig. 11. Water budgets for the Zhujiang River Estuary. The water flux is in 10^6 m³/d. V_Q, V_P, V_E, V_R and V_X are the river discharge, precipitation, evaporation, the residual flow and the mixing flow between the system of interest and the adjacent system, respectively. The words a and b refer to May and August 2015 cruises, respectively.

in the water column (Cloern, 1987; David et al., 2005; Liu et al., 2018), especially in the upper estuary with high turbidity. There exists a turbidity maximum zone near the four outlets (Wai et al., 2004). Phytoplankton growth was primarily light-limited due to high SPM concentrations (on average 32.5 mg/L) during the study period which reduced light levels. Our results agreed with previous reports that phytoplankton growth was primarily limited by light in the ZJRE (Shen et al., 2011; Li et al., 2017). Excess N was transported to the coastal waters of the ZJRE and the shelf of the northern SCS.

Eutrophication mitigates the levels of DO in the bottom waters of estuaries and leads to large area of hypoxia (Harrison et al., 2008). Low DO (<2 mg/L) in the surface water in the upper reach of the ZJRE is observed (Dai et al., 2006; He et al., 2014; Fig. 8). Recent studies have confirmed that nutrient enrichment leads to eutrophication over large area (several thousand square kilometer) in the transition region between the lower ZJRE and the adjacent shelf of the SCS (Lu et al., 2018; Zhao et al., 2020). Zhao et al. (2020) pointed out that 45%±13% of the eutrophication-driven production of organic matter in the plume fuels oxygen consumption, which is the most likely responsible for hypoxia in the coastal transition zone between the lower ZJRE and the adjacent continental shelf off Hong Kong (Qian et al.,2018; Li et al., 2020).

Table 4. Estimation of riverine fluxes to Zhujiang River Estuary and export nutrient fluxes (10^6 mol/d) of the Zhujiang River Estuary during May and August, 2015

	May 2015				August 2015			
	$F_{NO_3^-}$	F_{DIN}	F_{DIP}	F_{DSi}	$F_{NO_3^-}$	F_{DIN}	F_{DIP}	F_{DSi}
Riverine flux (VC)	71.5	108	0.75	145	75.4	91.1	0.78	170
Residual flow (V_RC_R)	–63.3	–77.6	–0.50	–31.1	–44.5	–51.1	–0.49	–47.7
Mixing exchange (V_XC_X)	–57.5	–71.7	–0.55	–28.6	–27.3	–29.3	–0.37	–12.3
Export flux ($V_RC_R + V_XC_X$)	121	149	1.05	59.7	71.8	80.4	0.86	60.0
Δ = (export flux – riverine flux)	–49.3	–46.7	–0.30	85.3	3.60	10.7	–0.08	110

Note: V_RC_R denoted residual nutrient transport out of the Zhujiang River Estuary; V_XC_X: mixing exchange flux of nutrients. Nutrient fluxes from the Zhujiang River Estuary to the South China Sea (seaward export flux) were estimated as the sum of the V_RC_R and V_XC_X. Positive and negative values of Δ indicate that other processes may magnify or reduce the riverine fluxes.

4 Conclusions

The river discharge played an important role in regulating riverine fluxes of DIN and DSi. Humen Outlet is the main path that riverine nutrient transported to the ZJRE. The box model results indicated that the export fluxes of phosphate out of the ZJRE were higher than the fluxes of riverine phosphate to ZJRE in May and August due to the influence of local sewage. Meanwhile, local sewage also led to higher export fluxes of DIN out of the ZJRE than fluxes of riverine DIN in May. Large amounts of DSi would be buried in the estuary in May and August. However, large amounts of nutrients transported to the ZJRE did not induce massive algal blooms due to the influence of light limitation.

Acknowledgements

We thank colleagues for their help with sampling.

References

Beck A J, Rapaglia J P, Cochran J K, et al. 2008. Submarine groundwater discharge to Great South Bay, NY, estimated using Ra isotopes. Marine Chemistry, 109(3–4): 279–291, doi: 10.1016/j.marchem.2007.07.011

Billen G, Garnier J. 2007. River basin nutrient delivery to the coastal sea: assessing its potential to sustain new production of non-siliceous algae. Marine Chemistry, 106(1–2): 148–160, doi: 10.1016/j.marchem.2006.12.017

Cai Weijun, Dai Minhan, Wang Yongchen, et al. 2004. The biogeochemistry of inorganic carbon and nutrients in the Pearl River Estuary and the adjacent northern South China Sea. Continental Shelf Research, 24(12): 1301–1319, doi: 10.1016/j.csr.2004.04.005

Cai Huayang, Huang Jingzheng, Niu Lixia, et al. 2018. Decadal variability of tidal dynamics in the Pearl River Delta: spatial patterns, causes, and implications for estuarine water management. Hydrological Process, 32(25): 3805–3819, doi: 10.1002/hyp.13291

Cloern J E. 1987. Turbidity as a control on phytoplankton biomass and productivity in estuaries. Continental Shelf Research, 7(11–12): 1367–1381, doi: 10.1016/0278-4343(87)90042-2

Cloern J E. 2001. Our evolving conceptual model of the coastal eutrophication problem. Marine Ecology Progress Series, 210: 223–253, doi: 10.3354/meps210223

Dai Minhan, Gan Jianping, Han Aiqin, et al. 2014. Physical dynamics and biogeochemistry of the Pearl River plume. In: Bianchi T, Allison M, Cai Weijun, eds. Biogeochemical Dynamics at Major River-Coastal Interfaces: Linkages with Global Change. New York: Cambridge University Press, 321–352

Dai Minhan, Guo Xianghui, Zhai Weidong, et al. 2006. Oxygen depletion in the upper reach of the Pearl River Estuary during a winter drought. Marine Chemistry, 102(1–2): 159–169, doi: 10.1016/j.marchem.2005.09.020

David V, Sautour B, Chardy P, et al. 2005. Long-term changes of the zooplankton variability in a turbid environment: the Gironde estuary (France). Estuarine, Coastal and Shelf Science, 64(2–3): 171–184, doi: 10.1016/j.ecss.2005.01.014

Fisher T R, Harding Jr L W, Stanley D W, et al. 1988. Phytoplankton, nutrients, and turbidity in the Chesapeake, Delaware, and Hudson estuaries. Estuarine, Coastal and Shelf Science, 27(1): 61–93

Gan Jianping, Lu Zhongming, Cheung Anson, et al. 2014. Assessing ecosystem response to phosphorus and nitrogen limitation in the Pearl River plume using the Regional Ocean Modeling System (ROMS). Journal of Geophysical Research: Oceans, 119(12): 8858–8877, doi: 10.1002/2014JC009951

Glibert P M, Wilkerson F P, Dugdale R C, et al. 2016. Pluses and minuses of ammonium and nitrate uptake and assimilation by phytoplankton and implications for productivity and community composition, with emphasis on nitrogen-enriched conditions. Limnology and Oceanography, 61(1): 165–197, doi: 10.1002/lno.10203

Gong Wenping, Lin Zhongyuan, Chen Yunzhen, et al. 2018. Effect of winds and waves on salt intrusion in the Pearl River Estuary. Ocean Science, 14(1): 139–159, doi: 10.5194/os-14-139-2018

Gordon Jr D C, Boudreau P R, Mann K H, et al. 1996. LOICZ biogeochemical modelling guidelines. LOICZ/R&S/95-5. Texel, Netherlands: LOICZ-IGBP

Guo Xianghui, Dai Minhan, Zhai Weidong, et al. 2009. CO_2 flux and seasonal variability in a large subtropical estuarine system, the Pearl River Estuary, China. Journal of Geophysical Research: Biogeosciences, 114(G3): G03013, doi: 10.1029/2008JG000905

Guo Zhanrong, Huang Lei, Liu Huatai, et al. 2008. The estimation of submarine inputs of groundwater to a coastal bay using Radium isotopes (in Chinese with English abstract). Acta Geoscientica Sinica, 29(5): 647–652

Hansen H P, Koroleff F. 1999. Determination of nutrients. In: Grasshoff K, Kremling K, Ehrhardt M, eds. Methods of Seawater Analysis. Weinheim, Germany: Wiley-VCH, 159–228

Harrison P J, Yin Kedong, Lee J H W, et al. 2008. Physical-biological coupling in the Pearl River Estuary. Continental Shelf Research, 28(12): 1405–1415, doi: 10.1016/j.csr.2007.02.011

He Biyan, Dai Minhan, Zhai Weidong, et al. 2014. Hypoxia in the upper reaches of the Pearl River Estuary and its maintenance mechanisms: a synthesis based on multiple year observations during 2000–2008. Marine Chemistry, 167: 13–24, doi: 10.1016/j.marchem.2014.07.003

Hu Jiatang, Li Shiyu. 2009. Modeling the mass fluxes and transformations of nutrients in the Pearl River Delta, China. Journal of Marine Systems, 78(1): 146–167, doi: 10.1016/j.jmarsys.2009.05.001

Hu Jiatang, Li Shiyu, Geng Bingxu, et al. 2012. Modeling of CBOD, TN and TP fluxes in the river network and estuary of Pearl River Delta. Journal of Hydraulic Engineering, 43(1): 51–59

Huang Xiaoping, Huang Liangmin, Yue Weizhong. 2003. The characteristics of nutrients and eutrophication in the Pearl River Estuary, South China. Marine Pollution Bulletin, 47(1–6): 30–36, doi: 10.1016/S0025-326X(02)00474-5

Jickells T D. 1998. Nutrient biogeochemistry of the coastal zone. Science, 281(5374): 217–222, doi: 10.1126/science.281.5374.217

Kot S C, Hu S L. 1995. Water flows and sediment transport in the Pearl River Estuary and wave in South China Sea near Hong Kong. In: Coastal Infrastructure Development in Hong Kong—A Review. Hong Kong, China: Hong Kong Government

Li Dou, Gan Jianping, Hui Rex, et al. 2020. Vortex and biogeochemical dynamics for the hypoxia formation within the coastal transition zone off the Pearl River Estuary. Journal of Geophysical Research: Oceans, 125(8): e2020JC016178, doi: 10.1029/2020JC016178

Li Ruihuan, Xu Jie, Li Xiangfu, et al. 2017. Spatiotemporal variability in phosphorus species in the Pearl River Estuary: influence of the river discharge. Scientific Reports, 7: 13649, doi: 10.1038/s41598-017-13924-w

Liang Cui, Xian Weiwei. 2018. Changjiang nutrient distribution and transportation and their impacts on the estuary. Continental Shelf Research, 165: 127–145, doi: 10.1016/j.csr.2018.05.001

Liu Jingqin. 2006. Investigation of distribution and influx calculation of nutrients in the Eight Pearl River Openings (in Chinese)[dissertation]. Qingdao: Ocean University of China

Liu Bo, de Swart H E, de Jonge V N. 2018. Phytoplankton bloom dynamics in turbid, well-mixed estuaries: a model study. Estuarine, Coastal and Shelf Science, 211: 137–151, doi: 10.1016/j.ecss.2018.01.010

Liu Sumei, Hong G H, Zhang Jing, et al. 2009. Nutrient budgets for large Chinese estuaries. Biogeosciences, 6(10): 2245–2263, doi: 10.5194/bg-6-2245-2009

Lu Zhongming, Gan Jianping. 2015. Controls of seasonal variability of phytoplankton blooms in the Pearl River Estuary. Deep-Sea Research Part II: Topical Studies in Oceanography, 117: 86–96, doi: 10.1016/j.dsr2.2013.12.011

Lu Zhongming, Gan Jianping, Dai Minhan, et al. 2018. Joint effects of extrinsic biophysical fluxes and intrinsic hydrodynamics on the formation of hypoxia west off the Pearl River Estuary. Journal of Geophysical Research: Oceans, 123(9): 6241–6259, doi: 10.1029/2018JC014199

Lu Fenghui, Ni Honggang, Liu Feng, et al. 2009. Occurrence of nutrients in riverine runoff of the Pearl River Delta, South China. Journal of Hydrology, 376(1–2): 107–115, doi: 10.1016/j.jhydrol.2009.07.018

Malakoff D. 1998. Death by suffocation in the Gulf of Mexico. Science, 281(5374): 190–192, doi: 10.1126/science.281.5374.190

McCarthy J J. 1981. The kinetics of nutrient utilization. In: Platt T, ed. Physiological Bases of Phytoplankton Ecology. Canadian Bulletin of Fisheries and Aquatic Sciences, 210: 211–233

Moore W S. 1996. Large groundwater inputs to coastal waters revealed by ^{226}Ra enrichments. Nature, 380(6575): 612–614, doi: 10.1038/380612a0

Nixon S W. 1995. Coastal marine eutrophication: a definition, social causes, and future concerns. Ophelia, 41(1): 199–219, doi: 10.1080/00785236.1995.10422044

Oudot C, Gerard R, Morin P, et al. 1988. Precise shipboard determination of dissolved oxygen (Winkler procedure) for productivity studies with a commercial system. Limnology and Oceanography, 33(1): 146–150, doi: 10.4319/lo.1988.33.1.0146

Parsons T R, Maita Y, Lalli C M. 1984. A Manual of Chemical and Biological Methods for Seawater Analysis. Oxford: Pergamon Press, 173

Qian Wei, Gan Jianping, Liu Jinwen, et al. 2018. Current status of emerging hypoxia in a eutrophic estuary: the lower reach of the Pearl River Estuary, China. Estuarine, Coastal and Shelf Science, 205: 58–67, doi: 10.1016/j.ecss.2018.03.004

Qu Hongjuan, Kroeze C. 2010. Past and future trends in nutrients export by rivers to the coastal waters of China. Science of the Total Environment, 408(9): 2075–2086, doi: 10.1016/j.scitotenv.2009.12.015

Rabalais N N, Turner R E, Sen Gupta B K, et al. 2007. Hypoxia in the northern Gulf of Mexico: does the science support the plan to reduce, mitigate, and control hypoxia?. Estuaries and Coasts, 30(5): 753–772, doi: 10.1007/BF02841332

Savchuk O P. 2005. Resolving the Baltic Sea into seven subbasins: N and P budgets for 1991–1999. Journal of Marine Systems, 56(1–2): 1–15, doi: 10.1016/j.jmarsys.2004.08.005

Shen Pingping, Li Gang, Huang Liangmin, et al. 2011. Spatio-temporal variability of phytoplankton assemblages in the Pearl River Estuary, with special reference to the influence of turbidity and temperature. Continental Shelf Research, 31(16): 1672–1681, doi: 10.1016/j.csr.2011.07.002

Strokal M, Kroeze C, Li Lili, et al. 2015. Increasing dissolved nitrogen and phosphorus export by the Pearl River (Zhujiang): a modeling approach at the sub-basin scale to assess effective nutrient management. Biogeochemistry, 125(2): 221–242, doi: 10.1007/s10533-015-0124-1

Tang Danling, Kester D R, Ni I H, et al. 2003. *In situ* and satellite observations of a harmful algal bloom and water condition at the Pearl River Estuary in late autumn 1998. Harmful Algae, 2(2): 89–99, doi: 10.1016/S1568-9883(03)00021-0

Turner R E, Rabalais N N. 1991. Changes in Mississippi River water quality this century: implications for coastal food webs. BioScience, 41(3): 140–147, doi: 10.2307/1311453

Turner R E, Rabalais N N. 1994. Coastal eutrophication near the Mississippi River Delta. Nature, 368(6472): 619–621, doi: 10.1038/368619a0

Wai O W H, Wang C H, Li Y S, et al. 2004. The formation mechanisms of turbidity maximum in the Pearl River Estuary, China. Marine Pollution Bulletin, 48(5–6): 441–448, doi: 10.1016/j.marpolbul.2003.08.019

Wang Jianing, Yan Weijin, Jia Xiaodong. 2006. Modeling the export of point sources of nutrients from the Yangtze River basin and discussing countermeasures. Acta Scientiae Circumstantiae, 26(4): 658–666

Wei Xing, Wu Chaoyu. 2014. Long-term process-based morphodynamic modeling of the Pearl River Delta. Ocean Dynamics, 64(12): 1753–1765, doi: 10.1007/s10236-014-0785-7

Xu Jie, Ho A Y T, He Lei, et al. 2012. Effects of inorganic and organic nitrogen and phosphorus on the growth and toxicity of two *Alexandrium* species from Hong Kong. Harmful Algae, 16: 89–97, doi: 10.1016/j.hal.2012.02.006

Xu Jie, Ho A Y T, Yin Kedong, et al. 2008a. Temporal and spatial variations in nutrient stoichiometry and regulation of phytoplankton biomass in Hong Kong waters: influence of the Pearl River outflow and sewage inputs. Marine Pollution Bulletin, 57(6–12): 335–348, doi: 10.1016/j.marpolbul.2008.01.020

Xu Jie, Yin Kedong, He Lei, et al. 2008b. Phosphorus limitation in the northern South China Sea during late summer: influence of the Pearl River. Deep-Sea Research Part I: Oceanographic Research Papers, 55(10): 1330–1342, doi: 10.1016/j.dsr.2008.05.007

Yin Kedong, Harrison P J. 2008. Nitrogen over enrichment in subtropical Pearl River estuarine coastal waters: possible causes and consequences. Continental Shelf Research, 28(12): 1435–1442, doi: 10.1016/j.csr.2007.07.010

Yin Kedong, Harrison P J, Goldblatt R H, et al. 1996. Spring bloom in the central Strait of Georgia: interactions of river discharge, winds and grazing. Marine Ecology Progress Series, 138: 255–263, doi: 10.3354/meps138255

Yin Kedong, Qian Peiyuan, Chen Jay C, et al. 2000. Dynamics of nutrients and phytoplankton biomass in the Pearl River Estuary and adjacent waters of Hong Kong during summer: preliminary evidence for phosphorus and silicon limitation. Marine Ecology Progress Series, 194: 295–305, doi: 10.3354/meps194295

Zhang Jing, Huang Weiwen, Létolle R, et al. 1995. Major element chemistry of the Huanghe (Yellow River), China-weathering processes and chemical fluxes. Journal of Hydrology, 168(1–4): 173–203, doi: 10.1016/0022-1694(94)02635-O

Zhang Ling, Wang Lu, Yin Kedong, et al. 2014. Spatial and seasonal variations of nutrients in sediment profiles and their sediment-water fluxes in the Pearl River Estuary, Southern China. Journal of Earth Science, 25(1): 197–206, doi: 10.1007/s12583-014-0413-y

Zhao Yangyang, Liu Jing, Uthaipan K, et al. 2020. Dynamics of inorganic carbon and pH in a large subtropical continental shelf system: interaction between eutrophication, hypoxia, and ocean acidification. Limnology and Oceanography, 65(6): 1359–1379, doi: 10.1002/lno.11393